Article

Tandem Synthesis of Furanaphthoquinones via Enamines and Evaluation of Their Antiparasitic Effects against *Trypanosoma cruzi*

Mariana F. C. Cardoso, [#,a] *Luana S. M. Forezi,* [#,a] *Acácio S. de Souza,* [a]
Ana F. M. Faria, [b] *Raissa M. S. Galvão,* [b] *Murilo L. Bello,* [c] *Fernando C. da Silva,* [a]
Robson X. Faria *,b,d *and Vitor F. Ferreira* *,e*

ᵃDepartamento de Química Orgânica, Instituto de Química, Universidade Federal Fluminense, 24210-141 Niterói-RJ, Brazil

ᵇPrograma de Pós-Graduação em Ciências e Biotecnologia, Departamento de Biologia, Instituto de Biologia, Universidade Federal Fluminense, 24210-141 Niterói-RJ, Brazil

ᶜLaboratório de Planejamento Farmacêutico e Simulação Computacional, Faculdade de Farmácia, Universidade Federal do Rio de Janeiro, 21941-599 Rio de Janeiro-RJ, Brazil

ᵈLaboratório de Avaliação e Promoção da Saúde Ambiental, Instituto Oswaldo Cruz (FIOCRUZ), 21045-900 Rio de Janeiro-RJ, Brazil

ᵉDepartamento de Tecnologia Farmacêutica, Faculdade de Farmácia, Universidade Federal Fluminense, 24241-000 Niterói-RJ, Brazil

Furanaphthoquinones are well known in medicinal chemistry for exhibiting relevant structural heterogeneity and bioactivities. In this work, it was synthesized a series of furanaphthoquinones through a tandem reaction between lawsone (**8**) and cyclic ketones in the presence of morpholine. This strategy provides an efficient and general method for synthesizing furanaphthoquinones with activity against the epimastigote form of *Trypanosoma cruzi* (*T. cruzi*), the parasite that causes Chagas disease. Compound **9b** was the better prototype, and it exhibited high potency for causing parasite death, showed reduced acute toxicity towards mammalian cells, and was capable of rupturing the epimastigote plasma membrane and acting on sterol 14α-demethylase (CYP51). Additionally, **9b** reduced trypomastigote viability by 99% after 24 h. Candidate **9b** demonstrated the best and most promising profile when bound to CYP51.

Keywords: quinones, lawsone, lapachones, Chagas disease, neglected diseases

Introduction

Medicinal chemistry has significantly contributed to the search for new drugs that can improve the quality of life of patients affected by various diseases. However, so-called neglected tropical diseases lack clinically effective drugs, and more research needs to be conducted to find new prototypes that can be transformed into drugs. Today, more than one billion people, one-sixth of the world's population, are suffering from neglected tropical diseases.[1] Chagas disease, caused by the protozoan *T. cruzi*, is a neglected tropical disease with high prevalence and

significant morbidity and mortality. The treatment of Chagas disease is still based on only two drugs, nifurtimox and benznidazole, both of which have limited efficacy in the late chronic phase, cause frequent side effects, and have evolved drug resistance.

In this context, naphthoquinones are considered promising structures in the field of medicinal chemistry, as their antitrypanosomal potential has been reported.[1] These compounds are associated with various biochemical processes in microorganisms such as fungi and bacteria and higher plants and animals. These compounds are involved in respiratory chain electron transport, energy production, coagulation, and blood cells. Naphthoquinone structural diversity and its similarities to endogenous molecules demonstrate that these compounds can treat and cure diseases caused by pathogenic microorganisms.[1-4] Research

groups have attempted to promote structural modifications in the naphthoquinone core in search of compounds with a better spectrum of action against *T. cruzi*. Thus, some naphthoquinones, such as **1-3**, and their derivatives, such as **4**, have been reported in the literature[5-9] to have activity against *T. cruzi* (Scheme 1a). Continuing our interest in the synthesis of naphthoquinones that can be used against *T. cruzi*, the etiologic agent of Chagas disease, we decided to study the reaction between lawsone (**5a**) and cyclic ketones **8** in the presence of morpholine to form furanaphthoquinones **9** via *in situ* formation of intermediate enamine (Scheme 1c). 1,4-Naphthoquinones can react with enamine **6** to produce furanaphthoquinone **7** (Scheme 1b).[10-14] However, enamines must be prepared in advance. This work describes a tandem reaction involving lawsone (**5a**), ketones (**8**), and morpholine, with the *in situ* formation of enamines, to produce furanaphthoquinones **9**; the trypanocidal activity of the new compounds against the epimastigote forms of *T. cruzi* was also evaluated.
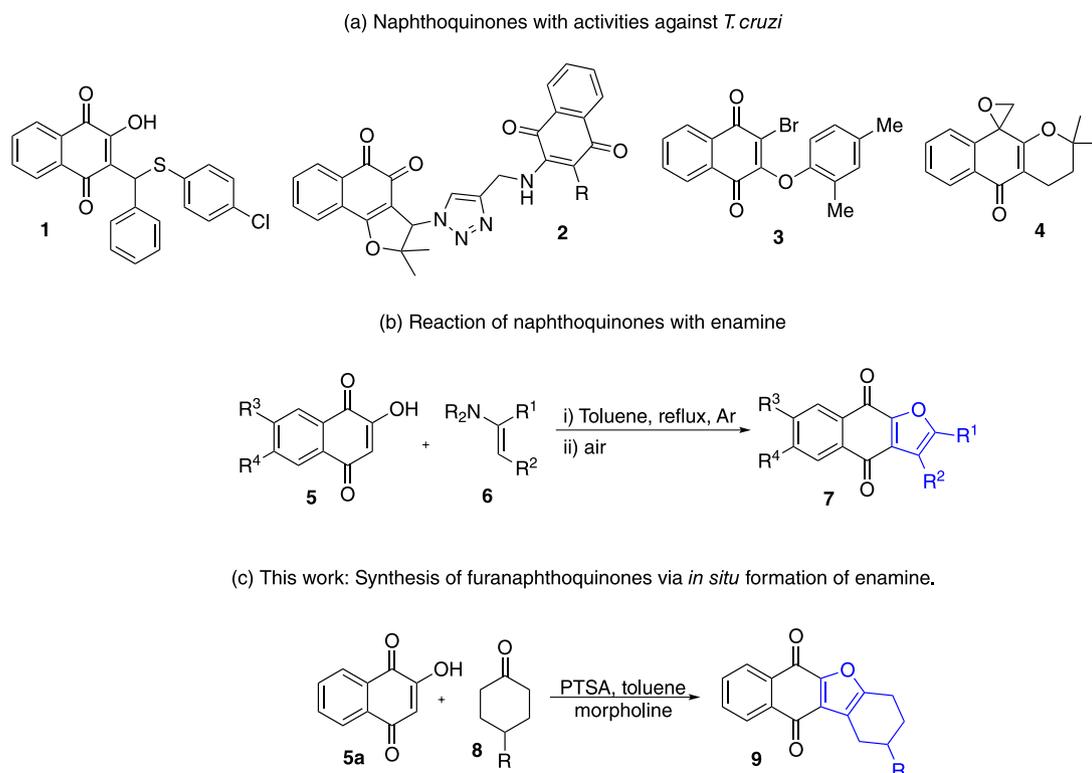
Experimental

Chemistry

Analytical grade solvents (Biograde, São Paulo, Brazil) were used. Column chromatography was performed using silica gel (SilicaFlash® P60 0.040-0.063 mm, Silicycle,

São Paulo, Brazil). Melting points (mp) were obtained on a Thermo Scientific 9100 apparatus (Waltham, USA) and were uncorrected. Infrared spectra (IR) were recorded on a Shimadzu IR Prestige-21 FTIR spectrometer (Kyoto, Japan) in KBr tablet (Sigma-Aldrich, São Paulo, Brazil). The reactor used to perform the reactions in the closed vessel was a Berghof model BR-300 (Eningen, Germany). ^{1}H and ^{13}C nuclear magnetic resonance (NMR) spectra were recorded at room temperature using a VNMRSYS-500 (Palo Alto, USA) or a Varian MR 300 instrument (Palo Alto, USA), using the solvents indicated, with tetramethylsilane (TMS) as the internal standard. Chemical shifts (δ) are given in ppm, and coupling constants (J) are given in hertz (Hz). High-resolution mass spectra (HRMS) were recorded on a MICROMASS Q-TOF mass spectrometer (Milford, USA).

General procedure for preparation of **9a-9c** and **10a-10c**

A 125 mL round bottom flask containing a solution of morpholine (11.4 mmol), ketone (**8**, 13.77 mmol), and *p*-toluenesulfonic acid (PTSA, 1.14 mmol) in toluene (40 mL) was refluxed for 5 h in a Dean-Stark apparatus. After this, 2-hydroxy-1,4-naphthoquinone (**5a**, 5.74 mmol) was added in portions, and reflux was maintained for more 2 h followed by another 12 h of stirring at room temperature. Then, the solvent was removed under reduced pressure, and

(a) Naphthoquinones with activities against *T. cruzi*

(b) Reaction of naphthoquinones with enamine

(c) This work: Synthesis of furanaphthoquinones via *in situ* formation of enamine.

Scheme 1. Some anti-*T. cruzi* naphthoquinones and synthesis of furanaphthoquinones from enamines.

the residue was purified by column chromatography on silica gel using a mixture of hexane:acetone as the gradient.

1,2,3,4-Tetrahydronaphtho[2,3-*b*]benzofuran-6,11-dione (**9a**)

Yellow solid (840 mg, 3.33 mmol, 58%); mp 195 197 °C; IR (KBr) ν / cm^{-1} 1656, 1639, 1619, 1584, 1573, 1500, 1402, 1218, 1160, 829; ^{1}H NMR (500.00 MHz, CDCl$_3$) δ 1.80-1.85 (2H, m), 1.90-1.95 (2H, m), 2.77 (2H, t, *J* 6.10 Hz), 2.82 (2H, t, *J* 6.30 Hz), 7.68-7.74 (2H, m), 8.12-8.14 (1H, m), 8.18-8.20 (1H, m); ^{13}C NMR (125.00 MHz, CDCl$_3$) δ 21.4, 22.3, 23.6, 118.8, 126.7, 129.5, 132.8, 133.5, 133.8, 142.2, 151.2, 159.9, 173.3, 182.2; HRESIMS *m/z*, calcd. for C$_{16}$H$_{12}$O$_3$Na$^+$ [M + Na]$^+$: 275.0679, found: 275.0680; Δ 0.4 ppm.

2-Methyl-1,2,3,4-tetrahydronaphtho[2,3-*b*]benzofuran-6,11-dione (**9b**)

Yellow solid (826 mg, 3.10 mmol, 54%); mp 187-189 °C; IR (KBr) ν / cm^{-1} 1687, 1649, 1618, 1584, 1583, 1478, 1400, 1214, 1150, 820; ^{1}H NMR (500.00 MHz, CDCl$_3$) δ 1.13 (3H, d, *J* 6.7 Hz), 1.22 (1H, s), 1.53-1.61 (2H, m), 2.32-2.38 (1H, m), 2.72- 2.86 (2H, m), 3.01 (1H, dd, *J* 16.7, 5.07 Hz), 7.68-7.74 (2H, m), 8.12-8.14 (1H, m), 8.18-8.20 (1H, m); ^{13}C NMR (125.00 MHz, CDCl$_3$) δ 21.1, 23.1, 28.9, 29.4, 30.3, 118.3, 126.7, 129.4, 132.8, 133.3, 133.5, 133.8, 151.4, 159.8, 173.3, 182.2; HRESIMS *m/z*, calcd. for C$_{17}$H$_{14}$O$_3$Na$^+$ [M + Na]$^+$: 289.0835, found: 289.0834; Δ 0.3 ppm.

2-(*tert*-Butyl)-1,2,3,4-tetrahydronaphtho[2,3-*b*]benzofuran-6,11-dione (**9c**)

Yellow solid (885 mg, 2.87 mmol, 50%); mp 207-209 °C; IR (KBr) ν / cm^{-1} 1694, 1656, 1614, 1588, 1582, 1477, 1405, 1212, 1160, 822; ^{1}H NMR (500.00 MHz, CDCl$_3$) δ 2.12-2.15 (1H, m), 2.36-2.39 (10H, m), 2.43-2.44 (1H, m), 2.65-2.72 (1H, m), 2.85-2.88 (1H, m), 2.98-3.02 (2H, m), 7.67-7.72 (2H, m), 8.10-8.11 (1H, m), 8.16-8.18 (1H, m); ^{13}C NMR (125.00 MHz, CDCl$_3$) δ 21.1, 23.9, 25.0, 27.2, 27.3, 28.4, 29.7, 112.3, 126.7, 128.1, 131.2, 133.8, 134.8, 136.4, 152.3, 157.0, 185.6, 185.9; HRESIMS *m/z*, calcd. for C$_{20}$H$_{20}$O$_3$Na$^+$ [M + Na]$^+$: 331.1305, found: 331.1288; Δ 5.1 ppm.

2-(Cyclohex-1-en-1-yl)-3-hydroxynaphthalene-1,4-dione (**10a**)

Orange solid (584 mg, 2.30 mmol, 40%); mp 230-233 °C; IR (KBr) ν / cm^{-1} 1699, 1691, 1653, 1650, 1628, 1614, 1588, 1454, 1430, 1217, 1203, 818; ^{1}H NMR (500.00 MHz, CDCl$_3$) δ 1.64-1.73 (4H, m), 2.16-2.21 (4H, m), 5.77 (1H, m), 7.61 (1H, td, *J* 7.5, 1.3 Hz), 7.69 (1H, td, *J* 7.56, 1.3 Hz), 8.03 (2H, ddd, *J* 15.6, 7.7, 1.0 Hz); ^{13}C NMR (125.00 MHz, CDCl$_3$) δ 22.6, 24.1, 26.0, 27.7, 114.5, 121.6, 125.5, 126.6,

127.6, 127.9, 130.8, 138.4, 144.3, 178.2, 182.8; HRESIMS *m/z*, calcd. for C$_{16}$H$_{14}$O$_3$Na$^+$ [M + Na]$^+$: 277.0835, found: 277.0822; Δ 4.7 ppm.

2-Hydroxy-3-(4-methylcyclohex-1-en-1-yl)-naphthalene-1,4-dione (**10b**)

Orange solid (585 mg, 2.18 mmol, 38%); mp 212-215 °C; IR (KBr) ν / cm^{-1} 1699, 1685, 1658, 1650, 1616, 1610, 1590, 1452, 1430, 1222, 1174, 821; ^{1}H NMR (500.00 MHz, CDCl$_3$) δ 1.05 (3H, s), 1.35-1.75 (6H, m), 5.01 (1H, d, *J* 7.8 Hz), 7.55-7.66 (2H, m), 7.95-7.99 (2H, m); ^{13}C NMR (125.00 MHz, CDCl$_3$) δ 21.3, 24.5, 26.7, 29.9, 43.4, 115.3, 126.1, 127.3, 127.8, 128.9, 129.5, 134.6, 140.6, 150.3, 184.8, 187.9; HRESIMS *m/z*, calcd. for C$_{17}$H$_{16}$O$_3$Na$^+$ [M + Na]$^+$: 291.0992, found: 291.0990; Δ 0.7 ppm.

2-(4-(*tert*-Butyl)cyclohex-1-en-1-yl)-3-hydroxynaphthalene-1,4-dione (**10c**)

Orange solid (749 mg, 2.41 mmol, 42%); mp 224-227 °C; IR (KBr) ν / cm^{-1} 1712, 1697, 1662, 1660, 1620, 1603, 1591, 1460, 1432, 1226, 1198, 837; ^{1}H NMR (500.00 MHz, CDCl$_3$) δ 0.84 (9H, s), 1.18 (1H, s), 1.30 (1H, ddd, *J* 24.5, 12.2, 4.8 Hz), 1.37-1.43 (1H, m), 1.83-1.87 (1H, m), 1.93-2.01 (1H, m), 2.15-2.22 (2H, m), 5.81-5.82 (1H, s), 7.61 (1H, td, *J* 7.5, 1.3 Hz), 7.69 (1H, td, *J* 7.6, 1.3 Hz), 8.03 (2H, ddd, *J* 16.1, 7.7, 0.8 Hz); ^{13}C NMR (125.00 MHz, CDCl$_3$) δ 22.4, 22.7, 22.9, 31.6, 33.9, 36.7, 48.2, 66.2, 116.4, 123.5, 127.5, 128.6, 129.5, 129.9, 132.8, 140.3, 146.3, 170.7, 178.4; HRESIMS *m/z*, calcd. for C$_{20}$H$_{22}$O$_3$Na$^+$ [M + Na]$^+$: 333.1461, found: 333.1446; Δ 4.5 ppm.

General procedure for preparation of **11a-11c**

To a 50 mL round bottom flask containing **10** (0.34 mmol), 10 mL of concentrated sulfuric acid was carefully added dropwise. The mixture was stirred at room temperature for 10 min and then poured onto ice, forming a precipitate in an aqueous medium. The suspension was extracted with ethyl acetate, the organic layer was dried with anhydrous sodium sulfate, and the solvent was removed under reduced pressure. The residue was purified by column chromatography on silica gel using hexane/ethyl acetate as the eluent.

7,8,9,10-Tetrahydronaphtho[1,2-*b*]benzofuran-5,6-dione (**11a**)

Red solid (58 mg, 0.23 mmol, 68%); mp 178-180 °C; IR (KBr) ν / cm^{-1} 1703, 1672, 1653, 1650, 1615, 1600, 1581, 1456, 1428, 1223, 1200, 832; ^{1}H NMR (500.00 MHz, CDCl$_3$) δ 1.58-1.68 (4H, m), 2.11-2.16 (4H, m), 7.57 (1H, td, *J* 7.5, 1.3 Hz), 7.64 (1H, td, *J* 7.5, 1.3 Hz), 7.98 (2H, ddd, *J* 15.7, 7.6, 1.0 Hz); ^{13}C NMR (125.00 MHz, CDCl$_3$)

δ 25.5, 26.3, 27.9, 29.7, 100.2, 118.0, 126.9, 129.3, 131.3, 132.8, 132.9, 134.9, 151.6, 159.7, 181.9, 184.0; HRESIMS *m/z*, calcd. for $C_{16}H_{12}O_3Na^+$ [M + Na]$^+$: 275.0679, found: 275.0671; Δ 2.9 ppm.

8-Methyl-7,8,9,10-tetrahydronaphtho[1,2-*b*]benzofuran-5,6-dione (**11b**)

Red solid (59 mg, 0.22 mmol, 65%); mp 155-157 °C; IR (KBr) ν / cm^{-1} 1722, 1680, 1668, 1655, 1612, 1605, 1577, 1450, 1421, 1217, 1206, 817; ^{1}H NMR (500.00 MHz, CDCl$_3$) δ 1.13 (3H, d, *J* 6.7 Hz), 1.40 (1H, dtd, *J* 13.3, 10.4, 5.5 Hz), 1.58 (1H, s), 1.85-1.90 (1H, m), 2.27 (1H, dddd, *J* 16.5, 9.3, 2.8, 2.0 Hz), 2.59-2.66 (1H, m), 2.75-2.85 (2H, m), 7.38 (1H, td, *J* 7.5, 1.5 Hz), 7.60 (2H, dtd, *J* 8.9, 7.6, 1.2 Hz), 8.01 (1H, dd, *J* 7.7, 0.6 Hz); ^{13}C NMR (125.00 MHz, CDCl$_3$) δ 25.5, 26.8, 28.7, 35.0, 39.7, 101.2, 117.8, 129.2, 130.9, 133.7, 135.3, 136.9, 138.6, 152.7, 158.7, 179.4, 184.5; HRESIMS *m/z*, calcd. for $C_{17}H_{14}O_3Na^+$ [M + Na]$^+$: 289.0835, found: 289.0827; Δ 2.8 ppm.

8-(*tert*-Butyl)-7,8,9,10-tetrahydronaphtho[1,2-*b*]benzofuran-5,6-dione (**11c**)

Red solid (65 mg, 0.21 mmol, 62%); mp 193-196 °C; IR (KBr) ν / cm^{-1} 1684, 1671, 1666, 1658, 1627, 1614, 1581, 1447, 1415, 1209, 1200, 821; ^{1}H NMR (500.00 MHz, CDCl$_3$) δ 1.81 (9H, s), 1.93 (1H, dd, *J* 24.7, 11.6 Hz), 2.18 (1H, d, *J* 11.2 Hz), 2.53-2.59 (1H, m), 3.00-3.04 (2H, m), 4.21-4.24 (1H, m), 4.38-4.44 (1H, m), 7.95 (2H, dtd, *J* 25.9, 7.4, 1.2 Hz), 8.30-8.33 (2H, m); ^{13}C NMR (125.00 MHz, CDCl$_3$) δ 28.8, 30.1, 31.7, 33.6, 38.3, 100.4, 116.7, 130.3, 131.8, 132.2, 133.0, 135.8, 136.7, 164.0, 169.2, 184.2, 191.6; HRESIMS *m/z*, calcd. for $C_{20}H_{20}O_3Na^+$ [M + Na]$^+$: 331.1305, found: 331.1301; Δ 1.2 ppm.

General procedure for preparation of **12a-12c**

A 50 mL round bottom flask containing a mixture of **9a-9c** (0.6 mmol), acetic anhydride (106 mmol), pyridine (3 drops) and Zn^0 (0.6 mmol) was incubated with stirring at room temperature for 4 days. Then, the mixture was filtered, and the solution was extracted with dichloromethane, washed with saturated sodium bicarbonate solution, and dried with anhydrous sodium sulfate. The solvent was then removed under reduced pressure.

1,2,3,4-Tetrahydronaphtho[2,3-*b*]benzofuran-6,11-diyl diacetate (**12a**)

Yellow solid (193 mg, 0.76 mmol, 95%); mp 223-225 °C; IR (KBr) ν / cm^{-1} 1698, 1693, 1659, 1655, 1611, 1591, 1588, 1464, 1415, 1218, 1169, 818; ^{1}H NMR (500.00 MHz, CDCl$_3$) δ 1.74-1.78 (2H, m), 1.84- 1.88 (2H, m), 2.30 (6H, s), 2.70 (2H, t, *J* 6.3 Hz), 2.75 (2H, t, *J* 6.3 Hz), 7.61-7.67 (2H, m), 8.05-8.06 (1H, m), 8.11-8.13 (1H, m); ^{13}C NMR (125.00 MHz, CDCl$_3$) δ 23.9, 32.6, 34.9, 117.4, 124.5, 126.5, 128.5, 130.9, 131.7, 133.8, 137.7, 141.3, 151.3, 160.9, 171.7, 183.3; HRESIMS *m/z*, calcd. for $C_{20}H_{18}O_5Na^+$ [M + Na]$^+$: 361.1046, found: 361.1043; Δ 0.8 ppm.

2-Methyl-1,2,3,4-tetrahydronaphtho[2,3-*b*]benzofuran-6,11-diyl diacetate (**12b**)

Yellow solid (341 mg, 0.97 mmol, 97%); mp 218-220 °C; IR (KBr) ν / cm^{-1} 1701, 1688, 1654, 1650, 1615, 1581, 1576, 1474, 1419, 1221, 1185, 830; ^{1}H NMR (500.00 MHz, CDCl$_3$) δ 1.06 (3H, d, *J* 6.6 Hz), 2.11-2.14 (1H, m), 2.19-2.21 (1H, m), 2.35-2.38 (1H, m), 2.43 (3H, s), 2.46 (3H, s), 2.71-2.75 (4H, m), 7.36-7.41 (2H, m), 7.77 (1H, dd, *J* 7.2, 2.0 Hz), 7.85 (1H, dd, *J* 7.1, 2.1 Hz); ^{13}C NMR (125.00 MHz, CDCl$_3$) δ 20.9, 22.9, 28.8, 29.2, 30.1, 30.3, 118.6, 126.6, 128.2, 129.3, 132.6, 133.2, 133.4, 133.6, 135.8, 151.3, 159.6, 173.1, 182.0; HRESIMS *m/z*, calcd. for $C_{21}H_{20}O_5Na^+$ [M + Na]$^+$: 375.1203, found: 375.1199; Δ 1.1 ppm.

2-(*tert*-Butyl)-1,2,3,4-tetrahydronaphtho[2,3-*b*]benzofuran-6,11-diyl diacetate (**12c**)

Yellow solid (218 mg, 0.55 mmol, 92%); mp 232-235 °C; IR (KBr) ν / cm^{-1} 1710, 1677, 1650, 1648, 1617, 1595, 1578, 1465, 1421, 1226, 1191, 828; ^{1}H NMR (500.00 MHz, CDCl$_3$) δ 1.13 (9H, d, *J* 6.7 Hz), 1.43 (1H, s), 1.53-1.61 (2H, m), 1.89-2.01 (2H, m), 2.32-2.38 (1H, m), 2.50 (6H, s), 3.01 (1H, dd, *J* 16.7, 5.1 Hz), 7.68-7.74 (2H, m), 8.12-8.14 (1H, m), 8.18-8.20 (1H, m); ^{13}C NMR (125.00 MHz, CDCl$_3$) δ 20.5, 20.8, 21.1, 22.8, 24.9, 26.0, 27.4, 29.8, 32.0, 40.1, 114.6, 121.7, 125.6, 126.7, 127.7, 128.1, 134.9, 138.5, 144.5, 168.1, 168.9, 177.1, 189.7; HRESIMS *m/z*, calcd. for $C_{24}H_{26}O_5Na^+$ [M + Na]$^+$: 417.1678, found: 417.1670; Δ 1.9 ppm.

General procedure for preparation of **13a-13c**

In a 600 mL high-pressure reactor (Berghof, Model BR-300), a solution in ethanol (200 mL) of **9** (4 mmol) and Pd/C (10 mol%) was stirred under 27 psi pressure of hydrogen for 10 min. Then, the mixture was filtered, and the solvent was removed under reduced pressure. The residue was purified by column chromatography on silica gel using hexane/ethyl acetate as the eluent.

6b,7,8,9,10,10a-Hexahydronaphtho[1,2-*b*]benzofuran-5,6-dione (**13a**)

Orange solid (356 mg, 1.40 mmol, 35%); mp 152-153 °C; IR (KBr) ν / cm^{-1} 1715, 1667, 1655, 1636, 1614, 1611,

1577, 1465, 1420, 1218, 1211, 820; ^{1}H NMR (500.00 MHz, CDCl$_3$) δ 1.69-1.75 (4H, m), 2.21-2.23 (4H, m), 2.91-2.94 (1H, m), 3.12-3.15 (1H, m), 7.65 (1H, td, J 7.5, 1.2 Hz), 7.73 (1H, td, J 7.6, 1.3 Hz), 8.07 (2H, ddd, J 16.1, 7.7, 0.8 Hz); ^{13}C NMR (125.00 MHz, CDCl$_3$) δ 21.8, 22.6, 25.5, 27.9, 56.9, 63.5, 118.1, 125.9, 126.9, 128.6, 132.8, 132.9, 134.9, 172.2, 181.9, 184.0; HRESIMS *m/z*, calcd. for $C_{16}H_{14}O_3Na^+$ [M + Na]$^+$: 277.0835, found: 277.0822; Δ 4.7 ppm.

8-Methyl-6b,7,8,9,10,10a-hexahydronaphtho[1,2-*b*]benzo-furan-5,6-dione (13b)

Orange solid (354 mg, 1.32 mmol, 33%); mp 141-143 °C; IR (KBr) ν / cm^{-1} 1703, 1664, 1660, 1650, 1620, 1611, 1581, 1449, 1425, 1210, 1206, 815; ^{1}H NMR (500.00 MHz, CDCl$_3$) δ 1.27 (3H, d, J 6.7 Hz), 1.50-1.58 (1H, m), 1.72 (1H, s), 1.99-2.04 (1H, m), 2.38-2.44 (1H, m), 2.73-2.80 (1H, m), 2.99-2.89 (2H, m), 2.87-2.77 (2H, m), 3.12-3.14 (1H, m), 3.32-3.35 (1H, m), 7.52 (1H, td, J 7.5, 1.5 Hz), 7.74 (2H, dtd, J 8.9, 7.6, 1.2 Hz), 8.15 (1H, dd, J 7.7, 0.6 Hz); ^{13}C NMR (125.00 MHz, CDCl$_3$) δ 21.5, 22.6, 24.7, 31.0, 35.7, 60.4, 66.6, 113.8, 125.2, 127.0, 129.7, 131.3, 132.9, 134.6, 170.3, 175.4, 180.5; HRESIMS *m/z*, calcd. for $C_{17}H_{16}O_3Na^+$ [M + Na]$^+$: 291.0992, found: 291.0977; Δ 5.1 ppm.

8-(*tert*-Butyl)-6b,7,8,9,10,10a-hexahydronaphtho[1,2-*b*]benzo-furan-5,6-dione (13c)

Orange solid (372 mg, 1.20 mmol, 30%); mp 174-177 °C; IR (KBr) ν / cm^{-1} 1720, 1671, 1659, 1651, 1625, 1613, 1588, 1453, 1420, 1215, 1212, 819; ^{1}H NMR (500.00 MHz, CDCl$_3$) δ 1.57 (9H, s), 1.65-1.72 (1H, m), 1.94 (1H, d, J 11.2 Hz), 2.29-2.35 (1H, m), 2.76-2.80 (2H, m), 3.75 (1H, d, J 7.7 Hz), 3.97-4.00 (1H, m), 4.14-4.20 (1H, m), 5.19 (1H, d, J 7.7 Hz), 7.71 (2H, dtd, J 25.9, 12.0, 7.4 Hz), 8.06-8.09 (2H, m); ^{13}C NMR (125.00 MHz, CDCl$_3$) δ 26.9, 28.1, 29.7, 31.6, 42.4, 60.8, 65.9, 114.7, 128.3, 129.8, 130.2, 131.0, 133.8, 134.7, 170.6, 177.6, 182.2; HRESIMS *m/z*, calcd. for $C_{20}H_{22}O_3Na^+$ [M + Na]$^+$: 333.1461, found: 333.1466; Δ 1.5 ppm.

Biological assays

Cell culture

Mouse peritoneal macrophages

These cells were obtained after peritoneal lavage from adult Swiss-Webster male mice (mass of 20-30 g). It was applied 10 mL of phosphate buffered saline (PBS) *per* animal, and the collected supernatant was centrifuged and plated. It was used animal breeding units in the Hélio and Pegy Pereira pavilions at FIOCRUZ/IOC under license number L039-2016.

Cultures of parasites

Epimastigote forms of *T. cruzi* (strain Y) were maintained in liver infusion tryptose (LIT) medium at 28 °C and through weekly passages. The mice were infected with trypomastigotes of *T. cruzi* obtained after metacyclogenesis in LIT medium at 28 °C to obtain the necessary parasite number for animal infection. The infected cells were maintained at 34 °C with CO$_2$. Parasites purified from the blood were resuspended in Dulbecco's modified Eagle's medium (DMEM) supplemented with 20% fetal bovine serum (FBS).

T. cruzi (Y strain - bloodstream trypomastigotes)

Trypomastigotes were obtained from the blood samples of infected albino Swiss mice at the peak of parasitemia. The purified parasites were resuspended in DMEM (Sigma-Aldrich, São Paulo, Brazil) supplemented with 10% FBS as reported previously.[8,9]

Vero cells were cultured in Roswell Park Memorial Institute (RPMI) medium supplemented with 5% FBS, 100 UI mL^{-1} antibiotic mixture, and 10 µg mL^{-1} streptomycin at 37 °C in an atmosphere of 5% CO$_2$ until the cells reached 90% confluence. The cell monolayer was infected with trypomastigotes (Y strain, 10 parasites *per* cell). After 24 h, the supernatant medium was collected, and Vero cells and amastigotes were removed by centrifugation at 1000 g for 5 min. Trypomastigotes were collected by centrifugation at 1600 g for 10 min.

Trypanocidal activity in trypomastigotes and amastigotes (Y strain) was determined using 1×10^6 cells mL^{-1} in 96-well plates and incubation at 37 °C for 24 h in the presence of the corresponding drug. Trypomastigote viability was determined by counting in a Neubauer chamber.

Cell metabolism activity test (Redox) *in vitro* using the resazurin reduction technique

Peritoneal macrophages derived from Swiss Webster strain mice were obtained through peritoneal lavage. The cell suspension contained in the supernatant was centrifuged at 1500 rpm for 5 min. The pellet was resuspended in 1 mL RPMI medium and counted in a Neubauer chamber. A total of 4×10^5 macrophages well^{-1} were seeded in triplicate in 96-well plates with RPMI medium supplemented with 10% FBS. These cells were incubated in an oven at 37 °C in a humidified atmosphere of 5% CO$_2$ for 24 h. After the cells adhered for 24 h, all the media was removed, and the compounds were added to plates in SFP-free (Shahidi Ferguson Perfringens free)

RPMI medium at 6 concentrations equal to 0.01, 0.1, 1, 25, 50, and 100 μM using a final volume of 200 μL well^{-1}. As a negative control, the wells were maintained only with cells and culture medium. It was used 0.5% Triton X-100 (Sigma-Aldrich, São Paulo, Brazil) as a positive control. The plates were incubated again for 24 h, and after that interval, the colorimetric assay was performed by reducing resazurin (RZ, Sigma-Aldrich, São Paulo, Brazil). A volume of 100 μL of the supernatant was removed from each well, and 20 μL of RZ (0.15 mg mL^{-1}) was added. The plates were incubated again for 4 h, and the readings were obtained in a spectrophotometer at 575 and 595 nm using SoftMax Pro software (version 5.1).[15] Data analysis was performed using GraphPad Prism 5.[16]

In vitro cell toxicity assay using the lactate dehydrogenase (LDH) release technique

After the treatment mentioned above in peritoneal macrophages, a volume of 50 μL was collected from each well and transferred to a new plate. A substrate mix prepared according to the manufacturer's specifications (Promega, Wisconsin, USA) was added and incubated for 30 min. After this time, the reaction stop reagent was added, and immediately afterwards, the absorbance was read in a spectrophotometer at 490 nm using SoftMax Pro software (version 5.1).[15]

Determination of trypanocidal action

The *T. cruzi* culture incubated for 24 h in LIT medium was added to a 96-well plate at 1×10^6 cells *per* 200 μL. It was added a 1 μM concentration of each compound and 20 μL of 0.2 μM propidium iodide solution for 30 min. The fluorescence was quantified as arbitrary fluorescence units of non-viable cells in a SpectraMax M4 spectrophotometer (Molecular Devices, California, United States of America) at 565-605 nm wavelengths. Triton X-100 (Sigma-Aldrich, São Paulo, Brazil) was used as a trypanocidal control, and the culture without compound addition was used as a negative control. All treatments were performed in triplicate.

Spectroscopic CYP51$_{TC}$ binding assay

Spectrophotometric titration was used for binding assays. A volume of 3 mL of 50 mM Tris-HCl (pH 7.5) and 10% glycerol was used in a UV-visible (UV-Vis) scanning spectrophotometer (Varian, Palo Alto, United States of America). The CYP51Tc (sterol 14α-demethylase from *T. cruzi*) concentration used was 0.1 μM. Stock solutions of **9a**, **9b**, **9c**, **11a** and **11b** were solubilized in dimethyl sulfoxide (DMSO, Sigma-Aldrich, São Paulo, Brazil) at 20 μM. Titrations were performed using a 3.5 mL quartz cuvette with a path length of 1 cm, and the inhibitor was added to 300 μL aliquots. As a negative control, DMSO was added in the same amounts, and the difference spectra were measured. KD (dissociation constant) values recorded for data titration of points were fitted to quadratic hyperbola using GraphPad Prism software (GraphPad Software Inc.),[16] as follows: A$_{obs}$ = (Amax/2 × Et){(S + Et + KD) − [(S + Et + KD)2 − 4 × S × Et]0.5}, where A$_{obs}$ is the absorption change determined at any inhibitor concentration, Amax is the maximal absorption shift recorded at saturation, KD is the dissociation constant for the inhibitor-enzyme complex, Et is the total enzyme concentration used, and S is the inhibitor concentration.

In silico

Molecular modeling of ligands

The compounds of the series **9-11** were initially built using the program Avogadro.[17,18] The geometry optimizations of molecules were then performed using the MMFF94 (Merck molecular force field 94). The optimized conformers were submitted to refinement calculations of the geometry optimization using the semiempirical parametric method PM6 performed by the MOPAC2016 program.[19]

Molecular docking

The program Molegro Virtual Docker (MVD)[20] was used to perform molecular docking (CLC Bio, 8200, Aarhus, Denmark). The MolDock score algorithm [GRID] with a grid resolution of 0.30 Å was selected as the score function, and the partial charges were assigned according to the MVD charge scheme. The MolDock Optimizer algorithm was used with a search space of 32 Å around the *T. cruzi* protein CYP51 structure. The CYP51 protein structure (PDB code: 4CK9) was retrieved from the Protein Data Bank (PDB). Molecular docking of the MC series compounds was performed using the same parameter set (runs = 100, population size = 50, max interactions = 2000, scaling factor = 0.50, and crossover rate = 0.90). The ligand poses were selected based on MolDock score values. Both the Molegro Virtual Docker[18] and PyMOL[21] were used to visualize and analyze the optimized molecular complexes.

Protein/ligand binding enthalpy

Molecular complexes of MC series compounds and *T. cruzi* 14-α-lanosterol demethylase (CYP51) obtained by docking and separate optimized ligands with protein before docking were applied to MOZYME calculation using a dielectric constant of 78.4. The calculations were performed using the MOPAC2016 program to indicate the molecular system heat of formation (ΔH$_f$).[17-23] Protein CYP51 and heme

group atom coordinates were fixed. For ligand molecules, geometry optimization was freely allowed.

Results and Discussion

Chemistry

Initially, through a reaction between 2-hydroxy-1,4-naphthoquinone (**5a**) and enamine, generated *in situ* from ketone **8** under acid catalysis of PTSA, we obtained a mixture of lapachone **9a**-**9b** and adduct **10a**-**10c** without the formation of furan-1,2-naphthoquinones **11a**-**11c**. However, when **10a**-**10b** were stirred in concentrated sulfuric acid for 10 min, it was obtained furan-1,2-naphthoquinones **11a**-**11c** in moderate yields (Scheme 2).

The possible mechanism of this reaction is stopped by the nucleophilic attack of enamine formed *in situ*, leading to intermediate **II** after oxidation of quinol and elimination of morpholine, resulting in furan-1,4-naphthoquinones **9a**-**9c**. This mechanism had already been reported by Kobayashi *et al.*[11] in a reaction between 2-hydroxy-1,4-naphthoquinones and previously synthesized enamines (Scheme 3).

The strategy used to improve the solubility of quinones in the biological environment, and therefore for them to be formulated to reach the biological target, is to transform them into diacetylated derivatives. Reichstein *et al.*[24] showed that metabolically labile furan-1,4-naphthoquinones were designed as prodrugs and were only slightly less active than their parent naphthoquinone counterparts in suppressing keratinocyte hyperproliferation in the micromolar range. In addition, Ma *et al.*[25] reported the preclinical evaluation of prodrug derivatives of β-lapachone encapsulated in biocompatible and biodegradable poly(ethylene glycol)-β-poly(D-lactic acid) (PEG-β-PLA) micelles. These formulations were used for the treatment of non-small cell lung cancers (NSCLC) that overexpress nicotinamide adenine dinucleotide phosphate (NAD(P)H):quinone oxidoreductase 1 (NQO1) and demonstrated efficiencies > 95% with significantly reduced hemolysis and methemoglobinemia that currently limits ARQ761 formulations.

To promote small changes in the furanaphthoquinone nucleus that transform the compounds into more soluble substances in biological media, reductive acetylation with acetic anhydride, zinc and pyridine was performed. As a
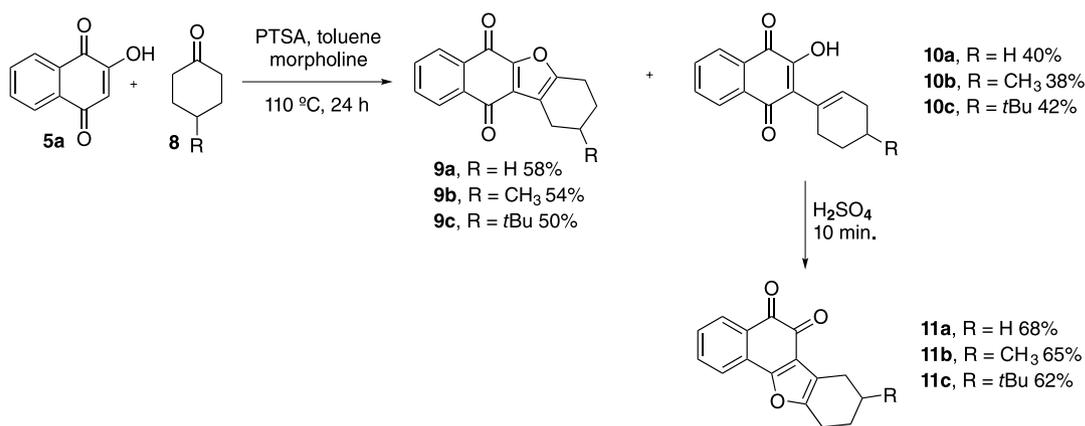
Scheme 2. Synthetic strategy for the preparation of furanaphthoquinones.
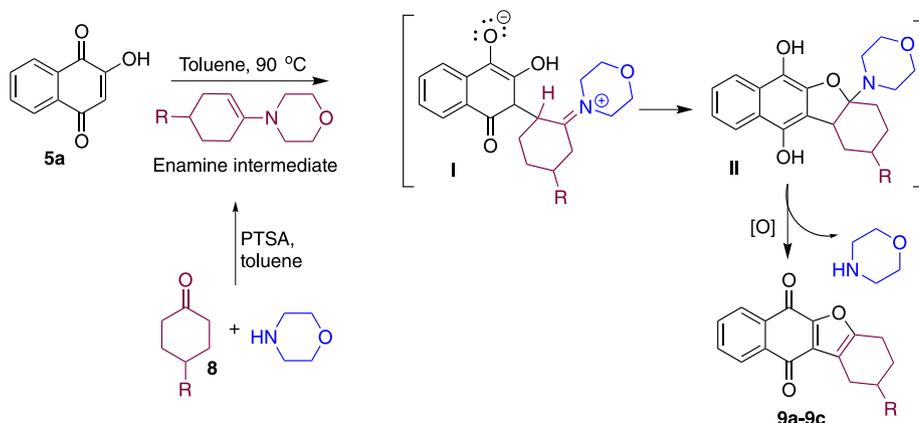
Scheme 3. Mechanistic proposal for obtaining furan-1,4-naphthoquinones.

result, acetylated derivatives **12a**-**12c** were obtained with excellent yields that ranged from 92 to 97% (Scheme 4). On the other hand, to investigate and compare the biological activity against *T. cruzi*, the catalytic hydrogenation of **9a**-**9c** to obtain **13a**-**13c** was performed in a reactor at 27 psi, and yields were low (30-35%) (Scheme 3). Finally, the structures of the new compounds were determined with ^{1}H NMR, ^{13}C NMR, and IR analysis in combination with mass spectrometry (see Supplementary Information section).

Biological assays

Cell viability

All naphthoquinone derivatives described were evaluated *in vitro* against *T. cruzi*. In the LDH release assay, the activity of this intracellular enzyme occurs when there is plasma membrane damage and subsequent cytoplasmic content leakage. In this scenario, after plasma membrane rupture, the cell dies from necrosis. Compounds **9a**-**9c**, **11a**-**11c**, **12a**-**12c**, and **13a**-**13c** at a concentration of 10 μM did not cause cellular toxicity. However, **10a**-**10c** caused toxicity after treatment for 24 h (Figure 1).

Trypanocide assays

The resazurin reduction assay was performed on epimastigotes of *T. cruzi* from the Y strain, which were treated for 72 h. Derivatives **9a**-**9c** and **11a**-**11c** at a concentration of 10 μM reduced parasite viability compared with non-treated parasites (CN). None of the treatments yielded activity higher than that of the positive controls, 0.05% Triton X-100 (CP) and 100 μM benznidazole (BZ, Sigma-Aldrich, São Paulo, Brazil). However, **9a**, **9b**, and **11b** exerted similar effects to BZ. All six derivatives reduced parasite viability by more than 75% compared with CN (Figure 2).

The cytotoxicity concentration (CC_{50}) estimated for the samples was determined after the treatments, and the concentrations ranged from 0.001 to 100 μM for 24 h. The CC_{50} values calculated for the derivatives were **9a** (32 μM), **9b** (177 μM), **9c** (107 μM), **11a** (56 μM) and **11b** (133 μM) (Figure 3). The results show low toxicity for all compounds. Derivatives **9c** and **11b** exhibited better results, with CC_{50} values greater than 100 μM. Other publication[26] exhibited naphthofuranquinone analogs with low toxicity compared with benznidazole. However, this furanaphthoquinone series produced via enamine yielded better non-toxic effects.

The half maximal effective concentration (EC_{50}) against epimastigote forms was obtained by ranging the concentrations from 0.01 to 100 μM for 72 h. The substances exhibited EC_{50} values of **9a** (0.1292 μM), **9b**
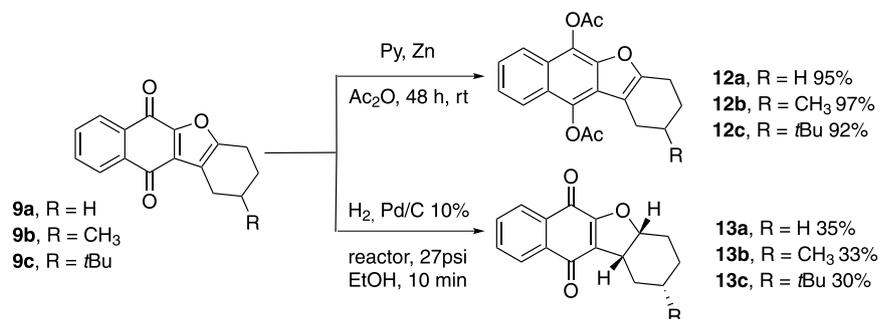
Scheme 4. Reductive acetylation and catalytic hydrogenation of furan-1,4-naphthoquinones.
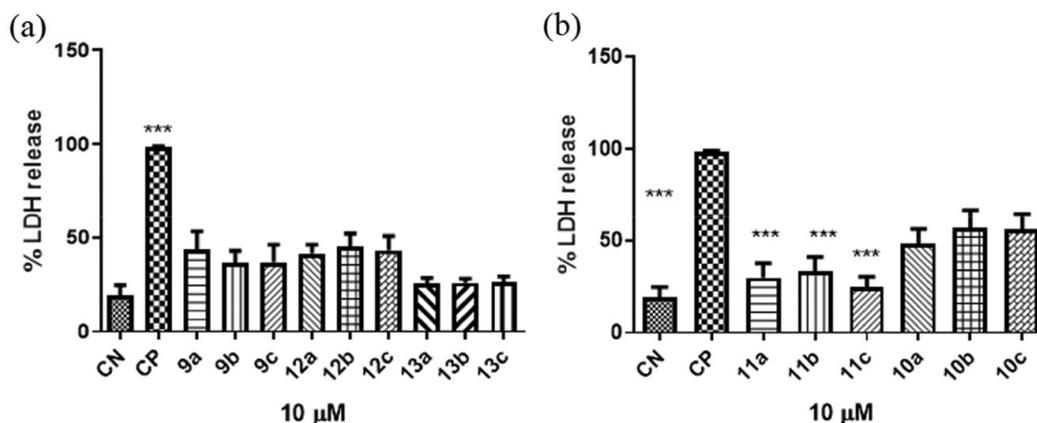

Figure 1. LDH release assay in peritoneal macrophages. Cell incubation for 24 h. This test was repeated three times on three separate days. CN: untreated cells; CP: cells treated with 0.05% Triton X-100. ***Denotes $p < 0.05$ compared to CN (negative control).
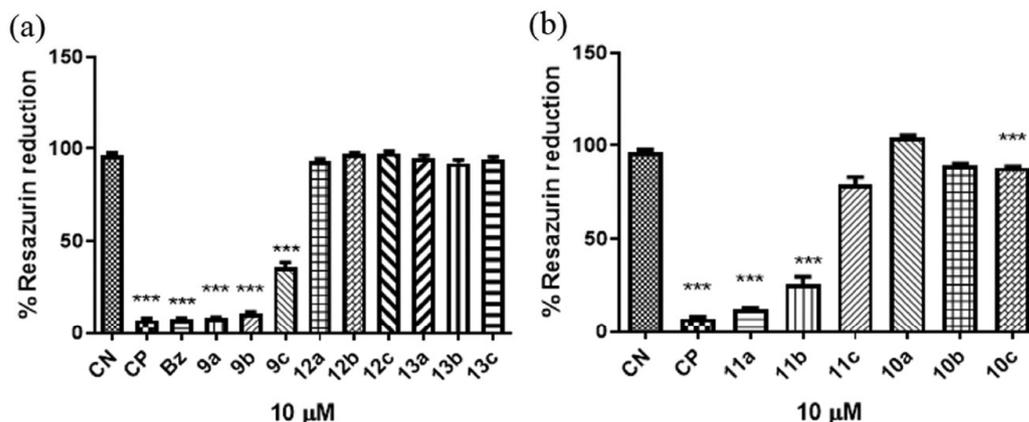
Figure 2. Cellular metabolic assay by reducing resazurin in *T. cruzi* Y strain epimastigotes. The parasites were treated for 72 h. This test was repeated four times on four different days. CN: untreated cells; CP: cells treated with 0.05% Triton X-100. ***Denotes $p < 0.05$ compared to CN (negative control).

(0.03118 μM), **9c** (0.03391 μM), **11a** (0.06437 μM) and **11b** (0.07447 μM) (Figure 4).
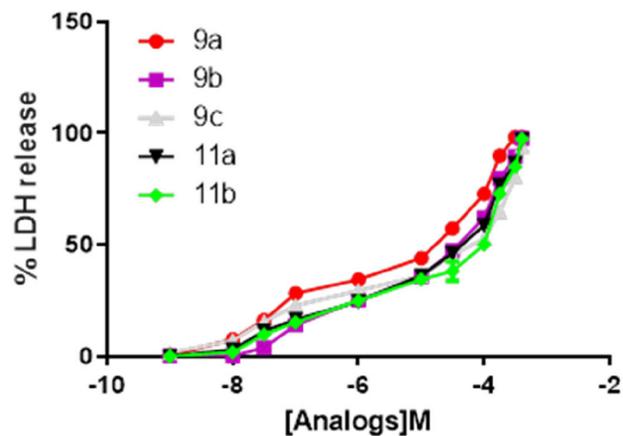
Figure 3. Compound toxicity in peritoneal macrophages. The cells were incubated for 24 h. This test was repeated in triplicate on three different days.
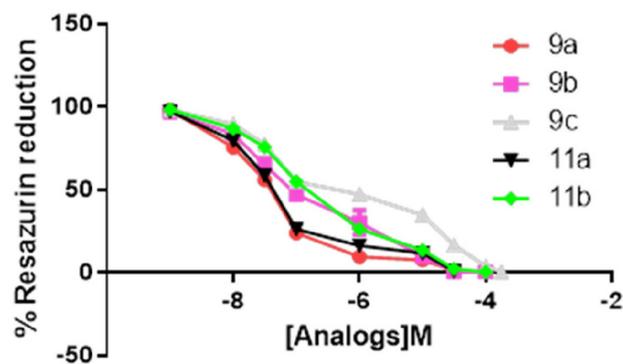
Figure 4. Compound toxicity evaluation in *T. cruzi* epimastigotes. The parasites were incubated for 72 h. This test was repeated in triplicate for three separate days.

The results obtained indicate that analogs with high potency affect parasite viability. Derivatives **9b** and **9c** were the most potent compared with other compounds. The IC_{50}

(half maximal inhibitory concentration) values for these analogs were in the range of 30 μM. These substances were tested against trypomastigote forms (Table 1). Treatment with 1 μM reduced trypomastigote viability compared to benznidazole. **9b** and **9c** produced the highest effects, reducing the parasite numbers by 99 and 95%. However, **11a** exhibited an effect similar to benznidazole. Additionally, **9a** and **11b** had worse effects than benznidazole.

Table 1. Results of the trypanocidal effect on trypomastigote forms

Compound	Trypomastigote death / %
Triton X-100 (0.5%)	100
Benznidazole (100 μM)	91 ± 1
9a	73 ± 6
9b	99 ± 0.6
9c	95 ± 3
11a	89 ± 4
11b	84 ± 2

In 2006, Silva *et al.*[27] described the trypanocidal activity of six naphthofuranquinones, and three of them exhibited IC_{50} concentration values ranging from 3-20 μM against epimastigote forms after 72 h. These substances caused trypomastigote mortality with IC_{50} values ranging from 158 and 641 μM within 24 h. In 2015, Cardoso *et al.*[26] presented prototype **13b** with IC_{50} values lower than 10 μM against trypomastigote forms in 24 h. Ferreira *et al.*[28] synthesized 16 analogs with IC_{50}/24 h in the range of 22-63 μM. Thus, the furanaphthoquinones contained in Table 1 exhibited satisfactory effect, reducing trypomastigotes by 73-99% at a concentration of 1 μM.

Selectivity index (SI)

We calculated the sample selectivity index based on the results described above and compared this index to that of

the reference drug benznidazole. Although the epimastigote form is infective for the intermediate host (barber), this index serves to indicate whether the sample has the potential to continue experiments in other forms or not. In general, molecules with SI below ten are considered insufficient to proceed in other forms of *T. cruzi*. All furanaphthoquinone-selected exhibited promising SI values. Compound **9b** demonstrated the best value (Table 2).

Table 2. EC_{50}, CC_{50} and selectivity index (SI) values

Drug	EC_{50} Y strain / μM	CC_{50} peritoneal macrophages (M0) / μM	SI
Benznidazole	17 ± 3	152 ± 6	938
9a	0.129 ± 0.011	32 ± 4	248
9b	0.031 ± 0,002	177 ± 4	5709
9c	0.033 ± 0.004	107 ± 8	3242
11a	0.064 ± 0.005	56 ± 3	875
11b	0.074 ± 0.006	133 ± 9	1794

Evaluation of trypanocidal action; M0: resting. EC_{50}: half maximal effective concentration; CC_{50}: cytotoxic concentration; SI: selectivity index.

In the propidium iodide (PI) uptake assay, we measured the fluorescence of this dye when the plasma membrane was damaged, and PI gained access to the nucleus and bound to DNA. This dye is positively loaded and has a size of 636 Daltons. Therefore, PI does not pass spontaneously through the plasma membrane. In this scenario, after plasma membrane rupture, the cell dies from necrosis-a usual scenario of trypanocidal drug action. However, treatment with a concentration of 1 μM increased PI fluorescence after 24 h of continuous treatment (Figure 5).

Thus, we investigated the binding affinities of all six analogs for CYP51 from *T. cruzi* (CYP51Tc). Sterol 14α-demethylase (CYP51) is a cytochrome P450 heme
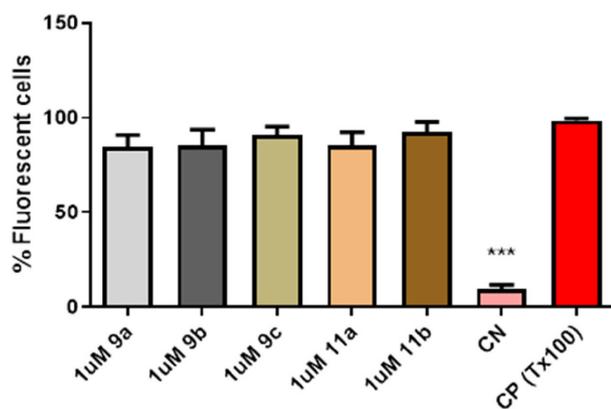
Figure 5. PI uptake assay in epimastigotes. The parasites were cultivated for 24 h. This test was repeated four times on four different days. CN: untreated cells; CP: cells treated with 0.05% Triton X-100. ***Denotes $p < 0.05$ compared to CN (negative control).

thiolate-containing enzyme associated with ergosterol and ergosterol-like biosynthesis and is a crucial membrane component in *T. cruzi*.[29-31] CYP51 activity may be impaired for azoles, resulting in cytostatic or cytotoxic effects.[32,33] Remarkably, the binding affinities of compounds **9a**, **9b**, **9c**, **11a** and **11b** to CYP51Tc were 0.07 ± 0.003, 0.02 ± 0.003, 0.03 ± 0.003, 0.04 ± 0.004, 0.06 ± 0.002, and 0.09 ± 0.002, respectively. The antifungal CYP51 inhibitor fluconazole was used as a reference and exhibited a value of 0.1 ± 0.09 (Figure 6). All analogs exhibited better affinity to bind with CYP51Tc than fluconazole. **9a** exhibits the most potent binding for **9c** and **11a**. Analogs **11b** and **9a** showed a moderate effect. In 2019, Dantas *et al.*[34] evaluated the anticancer activity of nor-β-lapachone tethered to 1*H*-1,2,3-triazole (1,2-FNQT) and observed partial inhibition of free radical scavenging activity and poor glycosidase inhibition.

In silico results

The furanaphthoquinone series compound molecular docking against *T. cruzi* was performed for the protein 14-α-lanosterol demethylase (CYP51). The results indicate that residues Ala115, Tyr116, and Leu98 appear essential for the affinity of compounds **9a**, **9b**, **9c**, **11a**, and **11b** to the molecular target. Furthermore, compounds **9a** and **9c** present similar conformational poses, showing the planar aromatic molecular moiety interacting with the heme group Fe atom by cation-π interactions. In addition, both compounds seem to form hydrogen bonds with the Tyr116 residue and hydrophobic interactions with residues Leu98 and Ala115 (Figure 7).

Compounds **11a** and **11b** exhibited similar poses. Both molecules show the planar aromatic molecular moiety interacting with the heme group Fe atom by cation-π interactions. Both compounds seem to form hydrogen bonds with the Tyr116 residue and with the heme group. Moreover, the molecular poses of both ligands **11a** and **11b** indicate hydrophobic interactions with residues Leu98 and Ala115 (Figure 7). However, the molecular docking result of compound **9b** indicates a different pose compared to **9a** and **9c**. For ligand **9b**, the molecular pose indicates that the intermolecular interactions are mainly hydrogen bonds and hydrophobic interactions. The hydrogen bond interaction is between the cyclic oxygen atom and Tyr116. The hydrophobic interactions are between the ring moieties of compound **9b** and the residues Leu98 and Ala115.

The heat of formation (ΔH_f) was calculated using ligands separated and complexed with protein CYP51 to indicate the affinity between interacting molecules
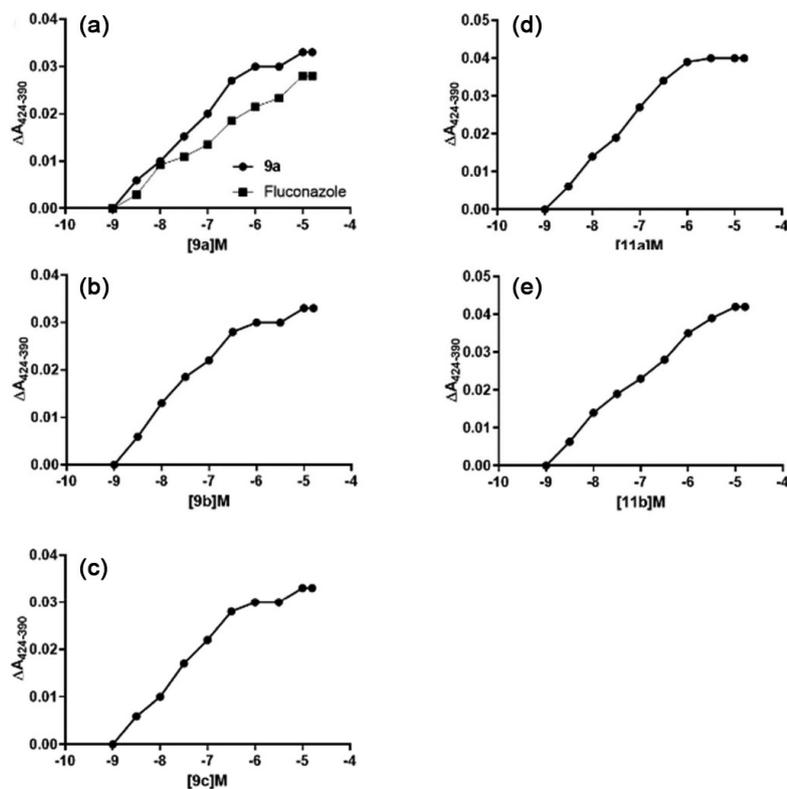
Figure 6. Furanaphthoquinones inhibit the CYP51 enzyme. (a) Compound **9a** and fluconazole; (b) **9b**; (c) **9c**; (d) **11a**; and (e) **11b** binding estimated from the absorption difference variation derived from the titration of CYP51Tc with increasing furanaphthoquinone analog concentrations. These experiments were performed in triplicate on two distinct days.
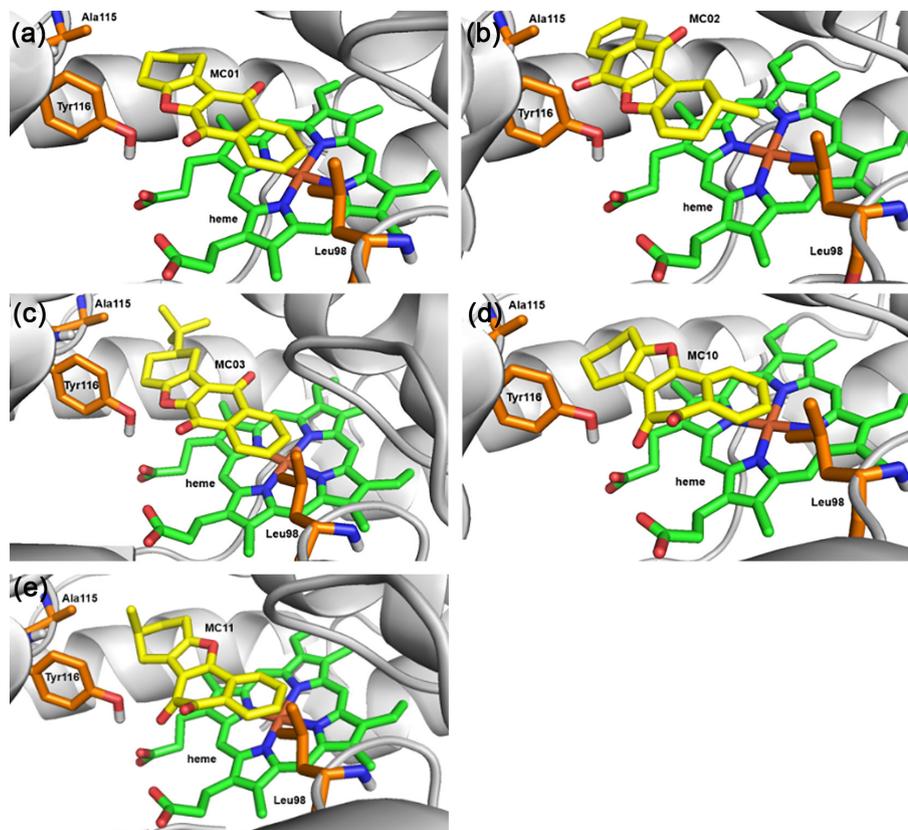
Figure 7. Molecular docking in 14-α-lanosterol demethylase (PDB code: 4CK9) for the furanaphthoquinone series compounds against *T. cruzi*. (a) **9a**; (b) **9b**; (c) **9c**; (d) **11a** and (e) **11b**.

(Table 3). The binding enthalpies of the studied ligands are different. The results indicate that **9b**, **9c**, and **11a** have more favorable binding enthalpies with *T. cruzi* CYP51.

Table 3. Heat of formation calculated for binding of the furanaphthoquinone series to *T. cruzi* 14-α-lanosterol demethylase (CYP51)

Molecular system	Heat of formation[a] / (kcal mol^{-1})
CYP51/**9a**	−11.97
CYP51/**9b**	−25.44
CYP51/**9c**	−20.90
CYP51/**11a**	−19.01
CYP51/**11b**	−17.52

[a]$\Delta H_f = \Delta H_f(\text{complex}) - \Delta H_f(\text{separate})$.

Conclusions

In summary, we have developed an operationally simple tandem synthetic protocol for the synthesis of six furanaphthoquinones by enamine intermediates in good yields. Analogs **9a**, **9b**, **9c**, **11a**, and **11b** exhibited potent and efficacious trypanocide activity against epimastigote forms. These analogs reduced trypomastigote viability by 75% within 24 h. All of these analogs exhibit trypanocide effects acting on the 14-α-lanosterol demethylase enzyme. Thus, these furanaphthoquinone series compounds represent promising candidates to potently and selectively eliminate *T. cruzi* with low toxicity.

Supplementary Information

Supplementary information is available free of charge at http://jbcs.sbq.org.br as PDF file.

Acknowledgments

Author Contributions

Mariana F. C. Cardoso was responsible for the organic synthesis work; Luana S. M. Forezi for the coordination of organic synthesis work, contributions to manuscript writing; Acácio S. de Souza for the organic synthesis work; Ana F. M. Faria, Raissa M. S. Galvão and Murilo L. Bello for the biological assays work; Fernando C. da Silva for the coordination of organic synthesis work, contributions to manuscript writing; Robson X. Faria for the coordination of biological assays, contributions to manuscript writing; Vitor F. Ferreira for the coordination of organic synthesis work, contributions to manuscript writing.

References

1. da Silva, F. C.; Ferreira, V. F.; *Curr. Org. Synth.* **2016**, *13*, 334.

2. Ahmadi, E. S.; Tajbakhsh, A.; Iranshahy, M.; Asili, J.; Kretschmer, N.; Shakeri, A.; Sahebkar, A.; *Mini-Rev. Med. Chem.* **2020**, *20*, 2019.

3. Janeczko, M.; Demchuk, O. M.; Strzelecka, D.; Kubiński, K.; Masłyk, M.; *Eur. J. Med. Chem.* **2016**, *124*, 1019.

4. Aminin, D.; Polonik, S.; *Chem. Pharm. Bull.* **2020**, *68*, 46.

5. Jentzsch, J.; Koko, W. S.; Al Nasr, I. S.; Khan, T. A.; Schobert, R.; Ersfeld, K.; Biersack, B.; *Chem. Biodiversity* **2020**, *17*, e1900597.

6. López-Lira, C.; Tapia, R. A.; Herrera, A.; Lapier, M.; Maya, J. D.; Soto-Delgado, J.; Oliver, A. G.; Lappin, A. G.; Uriarte, E.; *Bioorg. Chem.* **2021**, *111*, 104823.

7. González, A.; Becerra, N.; Kashif, M.; González, M.; Cerecetto, H.; Aguilera, E.; Nogueda-Torres, B.; Chacón-Vargas, K. F.; Zarate-Ramos, J. J.; Castillo-Velázquez, U.; Salas, C. O.; Rivera, G.; Vázquez, K.; *Med. Chem. Res.* **2020**, *29*, 665.

8. Bourguignon, S. C.; Cavalcanti, D. F. B.; Souza, A. M. T.; Castro, H. C.; Rodrigues, C. R.; Albuquerque, M. G.; Santos, D. O.; Silva, G. G.; da Silva, F. C.; Ferreira, V. F.; Pinho, R. T.; Alves, C. R.; *Exp. Parasitol.* **2011**, *127*, 160.

9. Bourguignon, S. C.; Castro, H. C.; Santos, D. O.; Alves, C. R.; Ferreira, V. F.; Gama, I. L.; da Silva, F. C.; Silva, W. S.; Pinho, R. T.; *Exp. Parasitol.* **2009**, *122*, 91.

10. Bian, J.; Deng, B.; Xu, L.; Xu, X.; Wang, N.; Hu, T.; Yao, Z.; Du, J.; Yang, L.; Lei, Y.; Li, X.; Sun, H.; Zhang, X.; You, Q.; *Eur. J. Med. Chem.* **2014**, *82*, 56.

11. Kobayashi, K.; Tanaka, K.; Uneda, T.; Maeda, K.; Morikawa, O.; Konishi, H.; *Synthesis* **1998**, 1243.

12. Kakisawa, H.; Tateishi, M.; *Bull. Chem. Soc. Jpn.* **1970**, *43*, 824.

13. Tateishi, M.; Kusumi, T.; Kakisawa, H.; *Tetrahedron* **1971**, *27*, 237.

14. Omote, Y.; Tomotake, A.; Kashima, C.; *J. Chem. Soc., Perkin Trans. 1* **1988**, 151.

15. *SoftMax Pro*, version 5.1; Molecular Devices, LLC, United States of America, 2010.

16. *GraphPad Prism*, version 5.00; GraphPad Software, Inc.; USA, 2008.

17. Cornell, T.; Hutchison, G.; *Avogadro*, version 1.1.2; University of Pittsburgh, USA, 2018.

18. Hanwell, M. D.; Curtis, D. E.; Lonie, D. C.; Vandermeersch, T.; Zurek, E.; Hutchison, G. R.; *J. Cheminform.* **2012**, *4*, 17.

19. *MOPAC2016*; Stewart Computational Chemistry, Colorado Springs, CO, USA, 2016, available at http://OpenMOPAC.net, accessed in October 2021.

20. *Molegro Virtual Docker*, version 6.0; Molexus IVS, Denmark, 2013.

21. The PyMOL Molecular Graphics System; *Pymol*, version 2.0; Schrödinger, LLC, USA, 2019.

22. Klamt, A.; Schüümann, G.; *J. Chem. Soc., Perkin Trans. 2* **1993**, 799.

23. Stewart, J. J. P.; *J. Mol. Model.* **2013**, *19*, 1.

24. Reichstein, A.; Vortherms, S.; Bannwitz, S.; Tentrop, J.; Prinz, H.; Müller. K.; *J. Med. Chem.* **2012**, *55*, 7273.

25. Ma, X.; Huang, X.; Moore, Z.; Huang, G.; Kilgore, J. A.; Wang, Y.; Hammer, S.; Williams, N. S.; Boothman, D. A.; Gao, J.; *J. Controlled Release* **2014**, *200*, 201.

26. Cardoso, M. F. C.; Salomão, K.; Bombaça, A. C.; Rocha, D. R.; da Silva, F. C.; Cavaleiro, J. A. S.; de Castro, S. L.; Ferreira, V. F.; *Bioorg Med. Chem.* **2015**, *23*, 4763.

27. Silva, R. S. F.; Costa, E. M.; Trindade, U. L. T.; Teixeira, D. V.; Pinto, M. C. F. R.; Santos, G. L.; Malta, V. R. S.; de Simone, C. A.; Pinto, A. V.; de Castro, S. L.; *Eur J. Med. Chem.* **2006**, *41*, 526.

28. Ferreira, S. B.; Salomão, K.; da Silva, F. C.; Pinto, A. V.; Kaiser, C. R.; Pinto, A. C.; Ferreira, V. F.; de Castro, S. L.; *Eur. J. Med. Chem.* **2011**, *46*, 3071.

29. Aoyama, Y.; *Front. Biosci.* **2005**, *10*, 1546.

30. Furlong, S. T.; *Exp. Parasitol.* **1989**, *68*, 482.

31. Roberts, C. W.; McLeod, R.; Rice, D. W.; Ginger, M.; Chance, M. L.; Goad, L. J.; *Mol. Biochem. Parasitol.* **2003**, *126*, 129.

32. Kolb, H. C.; Finn, M. G.; Sharpless, K. B.; *Angew. Chem., Int. Ed.* **2001**, *40*, 2004.

33. Wu, P.; Fokin, V. V.; *Aldrichim. Acta* **2007**, *40*, 7.

34. Dantas, R. F.; Senger, M. R.; Cardoso, M. F. C.; Ferreira, V. F.; de Souza, M. C. B. V.; da Silva, F. C.; Silva Jr., F. P.; *Med. Chem. Res.* **2019**, *28*, 1579.